

SUPPLEMENTAL MATERIAL:

MATERIALS AND METHODS

Cell culture. Human colorectal carcinoma HCT116 cells (ATCC, CCL-247) and CaCo2 (ATCC, HTB-37) were cultured in McCoy's 5a, or DMEM/F12 medium, respectively, supplemented with 10% fetal bovine serum (FBS) and 100 units/mL penicillin and 100 µg/mL streptomycin. Cells were maintained at 37°C in a humidified atmosphere and 5% CO₂. PMNs were isolated from human blood obtained from healthy volunteers by density gradient centrifugation (1) and handled according to protocols for the protection of human subjects, as approved by the Northwestern University Institutional Review Board. PMNs were used for experiments within 2h of isolation.

Antibodies and reagents. Anti-Ly6G Abs (clone 1A8) is from BD Biosciences (San Jose, CA, USA). Anti-CD11b (CBRM1/ 29) was purified in-house, mouse anti-LA/C (5G4), mouse anti-LB1/2 (2B2) (2); mouse anti-LC3, mouse anti-RAD50, mouse anti-TP53 (DO-1), mouse anti-Ku70 (Santa Cruz Biotechnology); rabbit anti-Ki67 (PC10), rabbit anti-MRE11, rabbit anti-pATR, rabbit anti-p-ATM (Cell signaling); rabbit anti-LB1 (3), rabbit anti-RAD51, rabbit anti-53BP1, rabbit anti-LA/C, mouse anti-CDKN1A (Abcam); mouse anti- γH2AX (JBW301), goat anti- γH2AX, rabbit anti-NBS1, goat anti-53BP1, rabbit anti-DNA-PKcs (R&D); mouse anti-GAPDH (FF26A/F9, Biolegend, Inc.).

Horseradish peroxidase conjugated anti-mouse/rabbit/goat (1 mg/mL; Jackson ImmunoResearch). Goat anti-mouse IgG-Alexa Fluor 488 and goat anti-rabbit IgG-Alexa Fluor 568 (Invitrogen). Chemotactic peptide formyl-methionyl-leucyl phenylalanine (fMLF) was from Sigma-Aldrich. Human/murine TNFα and IFNγ were from PeproTech (Rocky Hill, NJ, USA). Human recombinant MPO was purchased from Abcam. H₂O₂

ABTS, Camptothecin (CMPT), monodansylcadaverine (MDC) an endocytosis inhibitor and ROS scavengers N-acetyl-cysteine, NAC and Mn(III)tetrakis(4-benzoic acid)porphyrin (MnTBAP) were purchased from Sigma (St. Louis, MO). For *in vitro* use miR-23a/155 mimics and antagonist (ASO) (4-7) were purchased from Qiagen. For *in vivo* use Custom miRCURY LNA Power Inhibitor, mmu miR-23a/155, *in vivo* ready were purchased from EXIQON (Qiagen) (8-12)

Co-culture experiments. ~60% confluent human HCT116/CaCo2 cells were incubated with PMNs (2:1; two PMNs to one IEC), or PMN-MPs (4:1; MPs from four PMNs to one IEC) for 24-48 hours at 37°C in a humidified atmosphere and 5% CO₂. During long-term experiments, cells were maintained at 60% confluence, PMN-MPs were replaced every 48 hours. Population Doubling (PD) was calculated using the following equation: $PD = \log(N_h/N_s)/\log^2$, where N_h = number of harvested cells and N_s = number of seeded cells (13).

Colonoids generation. Colonic biopsies were obtained from consented, healthy patients (using 2.8mm Radial Jaw 4 Biopsy Cables, Boston Scientific) during routine screening procedures per approval by the Mayo Clinic IRB committee. Biopsied tissue was initially collected into Ringer's Solution, followed by cell dissociation by rocking the tissue in Gentle Cell Dissociation Reagent (Stemcell) for 30 min (40 rpm, RT). Biopsies were then further minced and triturated 20 times in DMEM/F12 with 1% BSA and passed through a 70µm filter to isolate colonic crypts. Colonic crypts were resuspended in equal parts of Intesticult Organoid Growth Medium and Matrigel Growth Factor Reduced Basement Membrane Matrix (Corning) and placed as domes in the center of four wells in a pre-

warmed 24-well dish. Formed matrigel domes were placed at 37° C for 10min to solidify in Intesticult Growth Medium supplemented with 10 μ M Y-27632 (Tocris) with 0.1 mg/mL Primocin (InvivoGen). Media was replaced every 3 days. Colonoids were passaged after reaching maturation (~10 days) by dissociation and replanting as above.

For gene, miRNA and protein expression analyses following PMN-MP treatment, colonoids were collected washed and treated as described in Supplemental material. For immunofluorescence, colonoids were frozen in OCT, sectioned into 10 μ m-width sections and treated with the appropriate primary followed by secondary Abs as detailed bellow.

Transmission electron microscopy. PMN-MPs were re-suspended in PBS, fixed by adding an equal volume of 2% PFA in 0.1 phosphate buffer (pH 7.4) to a final volume of 100 ml, and absorbed onto 400-mesh carbon-coated copper grids (10 min). Imaging was performed using an FEI Tecnai G2 Spirit transmission electron microscope.

Immunoblotting. Cell lysates were prepared by solubilization in Laemmli gel sample buffer (14). The protein concentration of samples was determined using BCA protein assay (Thermo Scientific). Equal amounts of protein from each sample were separated by SDS-PAGE on 10% gels and transferred to nitrocellulose. Peroxidase activity was detected using SuperSignal West Pico Chemiluminescence Detection kit (Thermo Scientific). Densitometry was performed using ImageJ.

Immunofluorescence. For clinical samples, paraffin-embedded healthy and IBD tissue sections were dewaxed, rehydrated and underwent epitope retrieval using protein-K buffer (15). For co-culture experiments, human PMN/PMN-MP/IECs were co-cultured on glass coverslips. For mouse tissue, cryosections (7-mm width) were prepared from the

extracted tissue that was frozen in optimum cutting temperature (OCT) compound (Sakura Finetek, Torrance, CA, USA). Tissue sections/coverlips were fixed in methanol (15 min at -20°C), permeabilized by 0.1% Triton X-100 in PBS (15 min at 22°C) and incubated with the relevant primary antibody (10 mg/ml, overnight at 4°C), followed by an appropriate fluorescently labeled secondary antibody (1h at room temperature). DNA was stained with 1 ng/ml Hoechst 33258 (Invitrogen). Coverslips were mounted on slides using ProLong™ Glass mountant (Thermo Fisher). All images were obtained using Zeiss LSM 510 microscope equipped with oil immersion objective lenses (PlanApochromat, 63X and 100X, 1.40 NA).

Gene expression analysis. Fresh IBD biopsies were obtained and handled as approved by the Northwestern University Institutional Review Board protocol. Mouse colonic wound tissue and the corresponding non-wounded regions were obtained using punch biopsies (2mm diameter). Total RNA from human clinical samples, cultured cells and mouse tissue was extracted by Trizol (Applied Biosystems), subjected to DNase I (Promega) treatment (3 U/mL reaction mixture), followed by an additional precipitation with Trizol. An ND-1000 Spectrophotometer (NanoDrop Technologies) was used to assess the quality and concentration of the RNA preparations. RT-PCR was carried out with the Applied Biosciences cDNA Synthesis kit (Thermo Scientific). For detection and quantitation of mature miRNA miScript PCR System (Qiagen) and miScript Primer Assay (Qiagen) were used. Gene expression analyses were performed on total cDNA using Roche SYBR Green Master Kit. The primers for gene- or miRNA-specific analysis by qRT-PCR were custom designed and obtained from IDT or Qiagen (QuantiTect Primer Assays kits). Primer sequences are available upon request. Relative expression analysis was carried out

using $2^{-\Delta\Delta CT}$ method with GAPDH serving as the reference gene. Data are shown as means of 4 independent experiments. A change in the expression of a specific gene was considered significant if the “fold change” was greater than 2.1 or less than 0.5.

COMET assay. To assess the presence of DSBs in IECs a COMET assay was performed according to manufacturer protocol (COMET SCGE kit Enzo, Trevigen). For mouse tissue, colonic wounds (day 4 post-wounding) and the corresponding non-wounded regions were extracted by punch biopsies (2 mm diameter). IECs were dissociated from the rest of the tissue by fragmentation and shaking in 1 mM EDTA/HBSS solution. Cultured murine and human IECs treated with PMNs, PMN-MPs or CMPT (10^5 cells/ml) were suspended in molten low melting temperature agarose (LMTA, 1:8; v/v), immobilized on glass slides and lysed in neutral buffer (0.5 M NaCl, 100 mM EDTA, 10 mM Tris, 2% sodium lauryl sarcosinate, 0.5% TritonX-100, 10% DMSO pH9.5 at 4°C). After washing (1× TBE; 90 mM Tris, 90mM boric acid and 2.5 mM EDTA, pH8.5), nuclei were separated by electrophoresis (10V, 50 min) (16). For DSB detection, slides were dehydrated with methanol, dried and DNA was stained with SYBR GREEN (Thermo Scientific). Images were obtained with a Zeiss LSM 510 microscope (PlanApochromat, 40X) and analyzed with the ImageJ plugin OpenComet.

BrdU labeling. Detection of DNA replication was carried out as described (13). Cells were incubated with 50 μ M BrdU (Sigma-Aldrich) in complete medium for 40 min at 37°C. BrdU-labeled DNA was detected with rat anti-BrdU (Sigma-Aldrich), followed by goat anti-rat IgG-Alexa Fluor 488 (Invitrogen) and analyzed using fluorescence-activated cell sorting (FACS) (BD LSRFortessa) or a Zeiss LSM 510 microscope using oil immersion objectives (PlanApochromat, 63X and 100X, 1.40 NA).

DNA ELISA. For detection of newly synthesized DNA: 1×10^6 cells were co-cultured with PMN/PMN-MPs in 10 cm dishes for 24h and incubated with $50 \mu\text{M}$ BrdU for 40 min at 37°C in a humidified atmosphere and 5% CO_2 . Genomic DNA was purified from cells using the QIAamp Blood Kit (QIAGEN). For detection of 8-OxoG in genomic DNA, ELISA procedure was adjusted using previously described protocols (17-20). BrdU and 8-OxoG detection were performed using 30 and 20 ng of genomic DNA, respectively. In each case, DNA samples were immobilized onto 96 well-plates using specific, mouse monoclonal BrdU (Abcam) and 8-OxoG (Trevigen) antibodies. The bound anti-BrdU/anti-8-OxoG antibodies were detected with peroxidase conjugated goat anti-mouse IgG (Zymed) and *o*-phenylenediamine (Sigma). The absorbance (OD) of reaction products was measured at 492 nm. BrdU in each sample was calculated as the ratio of ODs from each BrdU-labeled cell sample and DNA isolated from unlabeled cells. The fold increase of 8-OxoG was calculated as the ratio of ODs measured for DNA harvested after 24h treatment to DNA isolated from untreated cells. The experiments were repeated three times and the ELISA was performed in quadruplicate.

DNA fiber assays. For labeling with a single nucleoside, following treatment, IECs were incubated with $50 \mu\text{M}$ BrdU (Sigma-Aldrich) in complete medium for either 40 min or 2 hours at 37°C . For labeling with two nucleosides, IECs were first incubated with $50 \mu\text{M}$ CldU for 40 min at 37°C , PBS-washed, and treated with 4 mM hydroxyurea (HU) for 4 h at 37°C to induce replication fork stalling. Following HU treatment, IECs were washed three times with PBS and incubated with $50 \mu\text{M}$ IdU (40 min, 37°C). DNA fibers were prepared and stained as previously described (21). Briefly, single/double-labeled IECs were trypsinized, resuspended in ice-cold PBS (2×10^5 cells/ml), and mixed at ratio 1:10

with unlabeled cells. 3 μ l of the cell suspension was then mixed with 9 μ l of lysis buffer (0.5% SDS in 200 mM Tris-HCl, pH 7.4, 50 mM EDTA) on glass slides. After 5 min, slides were tilted gradually from 15° to 30° angle to spread the DNA fibers, air-dried and fixed in 3:1 methanol/acetic acid. Prior to labeling the DNA fibers, slides were dehydrated by incubation in 70% ethanol (overnight, 4°C), followed by incubation in ice-cold methanol (30 min, RT). DNA was denatured (2.5 M HCl, 1 h); slides were blocked for non-specific binding (by incubation in 3% BSA in PBS and 0.05% Tween 20) and incubated with the following antibodies (1h, RT): rat anti-BrdU that specifically detects CldU, and mouse anti-BrdU that detects IdU and does not cross-react with CldU (21). Secondary antibodies used to detect the anti-BrdU antibodies were goat anti mouse IgG-Alexa Fluor 488 and goat anti-rat IgG-Alexa Fluor 568 (Invitrogen). Images were obtained with a Zeiss LSM 510 Meta confocal microscope using oil immersion objective lenses (PlanApochromat, 63X and 100X, 1.40 NA).

Analysis of Double Strand Breaks repair. The repair of DSB by HR or NHEJ was analyzed using EGFP reconstitution vector system as previously described (22-24). Briefly, following the defined treatment, IECs were electroporated (GenePulser Xcell BioRad) with a plasmid mix containing 10 μ g of the *SceI* meganuclease expression plasmid (pCMV-I-*SceI*), and 10 μ g of one of the DSB repair substrates (*EJ-EGFP* or *HR-EGFP/3'EHGFP*) or 10 μ g of wild type *EGFP* plasmid (to determine transfection efficiency). Fluorescence signal due to incorporated EGFP, as an index of HR/NHEJ activity was quantified using Zeiss LSM 510 Meta confocal microscope (PlanApochromat, 40X; Sup Fig 2B). DSB repair frequencies were estimated as the

fraction of EGFP-positive cells and calibrated to the transfection efficiency, determined in parallel by EGFP control plasmid.

Cell cycle analysis. For cell cycle analysis, 1×10^6 IECs following PMN/PMN-MP treatment were collected by trypsinization, washed with PBS, and fixed in 100% ethanol. Fixed cells were treated with RNaseA and 0.1% Triton-X100 in PBS (3h, RT), stained with propidium iodide (PI) and analyzed by FACS (BD LSRFortessa) for cell cycle phases and aneuploidy. For PMN-IEC co-culture, IECs were separated from PMNs using additional staining for PMN marker Ly6G. Cell apoptosis was quantified using Annexin V and PI staining by FACS, as above.

Detection of Senescence Associated (SA)- β -gal activity. Senescence marker SA- β -gal was detected according to the manufacture-provided protocol using β -galactosidase activity assay (Sigma Aldrich).

All methods below have been approved by the Mayo Clinic IRB Committee. O Fresh IBD biopsies were obtained and handled as approved by the Northwestern University Institutional Review Board protocol.

Statistical analysis. Two-tailed student's t-test and One-way Anova was used for statistical analyses. All of the results presented are the mean \pm standard deviation from at least three separate experiments. Significance was set at p-value < 0.05 .

SUPPLEMENTAL FIGURES AND TABLE

Supplemental Figure 1. A. Low magnitude (40X), representative immunofluorescence images of healthy and IBD colon tissue sections shown in figure 1A, stained for LB1

(red) and γ H2AX (green) (left panels) and for LA/C (green) and CD11b (red) (right panels). **B.** Immunoblotting of PMNs and PMN-MP cultured without IECs for 24h (n=3). **C.** Cell cycle analysis by FACS of IECs cultured with PMNs with and without ROS scavenger, NAC, 2mM, 24h (n=4, ** p<0.001, ^{ns} not significant). **D.** An induction of apoptosis in IECs treated with PMN-MP was quantified by FACS following staining for Annexin V and propidium iodide (PI, n=3, ^{ns} not significant). **E.** Relative expression analysis of the indicated genes in IECs following 24h treatment with PMNs or PMN-MPs. Data shown as expression relative to not-treated IECs. GAPDH was used as a reference gene. **F.** Expression of the indicated proteins, including lower molecular weight bands, detecting cleavage products, were analyzed by immunoblotting following 24 and 48 hours of IECs and PMN-MP co-culture. LC3 is an autophagy marker and GAPDH was used as loading reference (n=4). **G.** β -gal expression as an index of IEC senescence was examined 24 and 48 hours following PMN or PMN-MP treatment, as described in methods (n=3, * p<0.05). **H.** ELISA detecting 8-OxoG in genomic DNA isolated from IECs treated with PMNs, PMN-MPs or recombinant MPO (2 μ g/ml) with its substrate, H₂O₂ (24h, n=4, ** p<0.01, *** p<0.001). **I.** Relative expression analysis of indicated genes following 24h IEC co-culture with PMNs or PMN-MPs. Data shown as expression relative to not-treated IECs. GAPDH was used as a reference gene (n=4, * p<0.05). **K.** Following treatment with PMN-MPs, IECs were incubated with BrdU for 40 min. BrdU was detected in isolated genomic DNA by ELISA as described in Supplemental Methods (n=4, DNA samples was assayed in quadruplicate; ** p<0.001). Two-tailed student's t-test and One-way Anova were used for statistical analyses (p values); data represent the mean \pm SD from at least three independent experiments.

Supplemental Figure 2. **A.** Kinetics of DSB repair in CMPT- and PMN-MP-treated IECs was determined by COMET assay, as described in methods. Over 1000 nuclei/time point/condition were analyzed (n=4). **B.** Representative images of EGFP expression analysis induced by activation of HR or NHEJ. **C.** Expression of the indicated DDR proteins were quantified by immunoblotting, following 24 and 48h of IECs and PMN-MP co-culture. GAPDH was used as loading reference (n=4). **D.** Relative mRNA expression analysis of the indicated genes following 24h IEC co-culture with PMNs or PMN-MPs. Data shown as expression relative to not-treated IECs. GAPDH was used as a reference gene. (n=4). **E.** Analyses of LB1 interactions with RAD51 promoter by ChIP-qPCR. The fraction of LB1 that was associated with nuclear chromatin was immunoprecipitated using specific LB1 antibody from PMN-MP treated IECs at indicated time points. An input and the precipitated DNA samples were analyzed by qPCR (n=4, with 5 technical repeats). **F.** Electrophoresis of isolated PMN genomic DNA (5×10^5 cells) before and after DNase I treatment (5 U/ml, 30 min). **G.** PMN-MPs (isolated from fMLF-stimulated PMNs) were treated with DNase I (5 U/ml, 30 min) with/without permeabilization by NP40. The relative expression of miR-23a/-155 was determined by qRT-PCR. Data shown as fold increase over control PMN-MPs (isolated from unstimulated PMNs). U-6 was used as a reference gene (n=8, ** p<0.01). **H.** Gene expression analysis and **I.** Immunoblotting of LB1, RAD51 and DSB marker, γ H2AX, in PMN-MP treated IECs with/without PMN-MP pre-treatment with DNase I (5 U/ml, 30 min) (n=8, * p<0.05). **J.** Quantification of immunoblotting analyses (shown in Fig 4C) of IECs treated with PMN-MPs (24h) and/or RNase pre-treatment (10 μ g/ml, 45 min), addition of miR-23a/155 mimics/ASOs (1 nM each; n=3). Quantification was performed using Li-COR odyssey

densitometry software (Li-Cor). Two-tailed student's t-test and One-way Anova were used for statistical analyses (p values); data represent the mean \pm SD from at least three independent experiments.

Supplemental Figure 3. A. Relative expression analysis of the indicated genes and miRNAs in IECs following treatment (24h) with control MPs (derived from non-activated PMNs, NA) or PMN-MPs derived from fMLF-stimulated PMNs. Where indicated, IECs were pretreated with the endocytosis inhibitor, MDC (50 μ M, 45 min). Data shown relative to not treated IECs. U-6 was used as a reference gene for miRNAs and GAPDH for gene expression (n=3, *** p<0.001, n.s.- not significant). **B.** FACS analysis for PMN (Ly6c^{hi}/Ly6G^{hi}), monocyte (Ly6c^{hi}/Ly6G⁻) and inflammatory macrophage (Ly6c^{hi}/CD64⁺) infiltration of IECs in colonic wounds. IECs were extracted from colonic wounds at day 2 post-injury and prepared for FACs as described in Supplemental Methods. **C.** Tissue MPs were isolated from extracted colonic wounds, with/without PMN depletion at day 2 post-injury and analyzed for miR-23a and-155 expression by qRT-PCR. Data shown as expression relative to non-wounded tissue. U-6 was used as a reference gene. (n=3, ** p<0.001). **D.** The relative expression of LA/C and LB2 in colonic wounds following Scr or miR-23/155 ASOs treatment (72h) was determined by qRT-PCR. Data are shown as fold change relative to non-wounded and not treated tissue. GAPDH was used as a reference gene. (n=4, ^{ns} not significant). Two-tailed student's t-test and One-way Anova were used for statistical analyses (p values); data represent the mean \pm SD from at least three independent experiments.

Supplemental Figure 4. Patient-derived colonoids grown in 3D cultures were treated with PMN-MPs (24h, derived from fMLF-stimulated PMNs). **A.** Relative expression

analysis of pri-miR-23a/155 following PMN-MP treatment. Data shown as fold increase over control, not-treated colonoids. GAPDH was used as a reference gene. (n=3). **B.**

Representative immunofluorescence images of LB1 nuclei staining (red) as analyzed by confocal microscopy to detect changes in the nuclear organization.

C. Micronuclei were identified by parallel DAPI nuclei staining and a DSB marker γ H2AX. **D.** Relative expression analysis of the indicated genes in colonoids following PMN-MP treatment. Data shown relative to not-treated colonoids, using GAPDH as reference gene (n=3, * p<0.05). Two-tailed student's t-test and One-way Anova were used for statistical analyses (p values); data represent the mean \pm SD from at least three independent experiments.

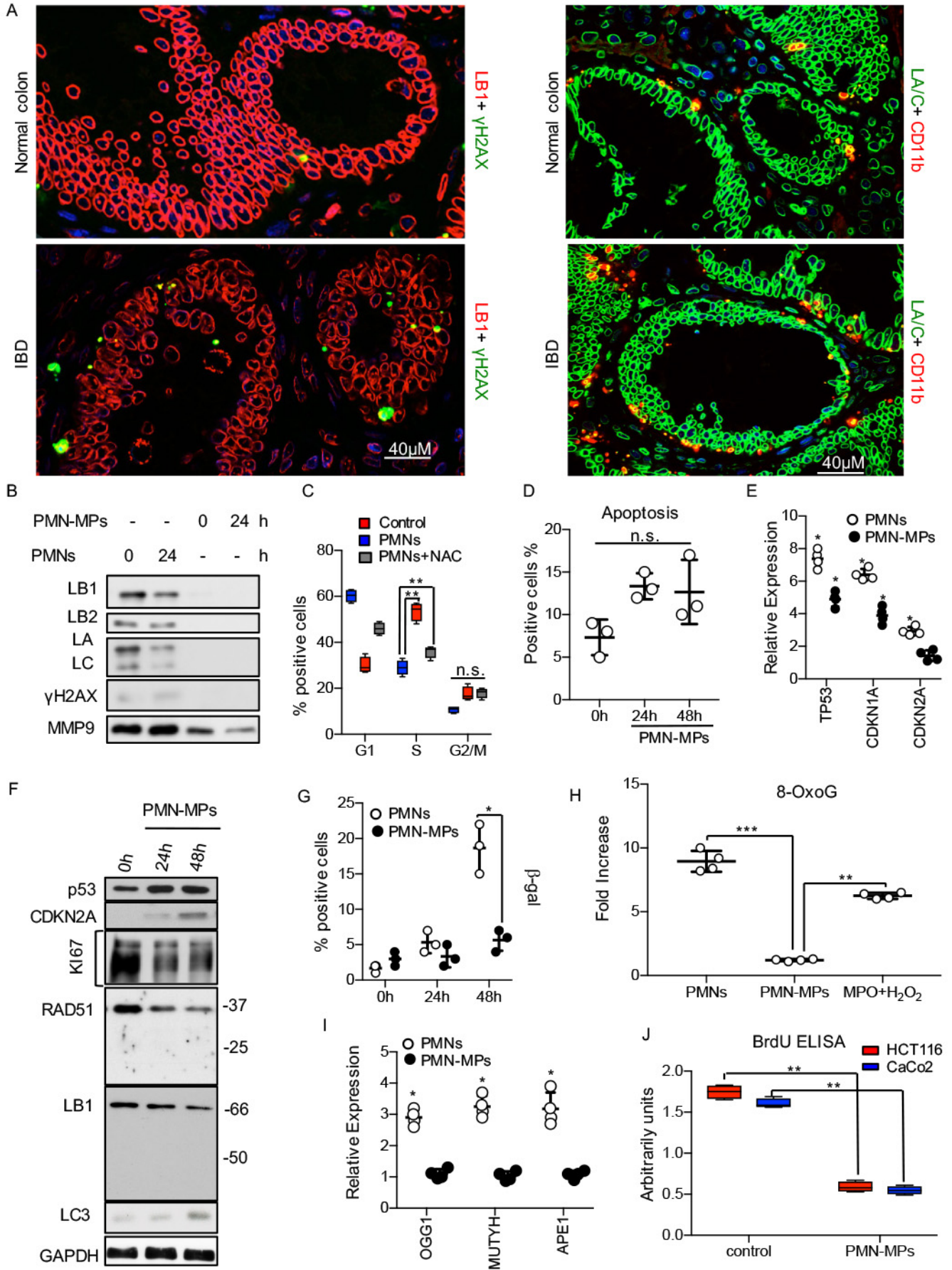
Supplemental Table 1. Expression of DNA damage repair regulating miRNA by PMN and PMN-MPs. Expression analyses of pro-inflammatory miRNAs associated with detection and repair of DNA damage were performed by qRT-PCR for the following conditions: 1. fMLF-stimulated PMNs (1 μ M, 20 min, 37⁰ C), 2. MPs isolated from fMLF-stimulated PMNs, 3. Fresh clinical biopsies of active IBD (A) and healthy (non-inflamed, NA) colon tissue. U-6 was used as a reference gene. GAPDH was used as a reference gene for quantitation of pri-miR-23a/155. Significance was set if expression change was > 2.1 or < 0.5. All of the results presented are the mean \pm standard deviation from at least three separate experiments.

Reference:

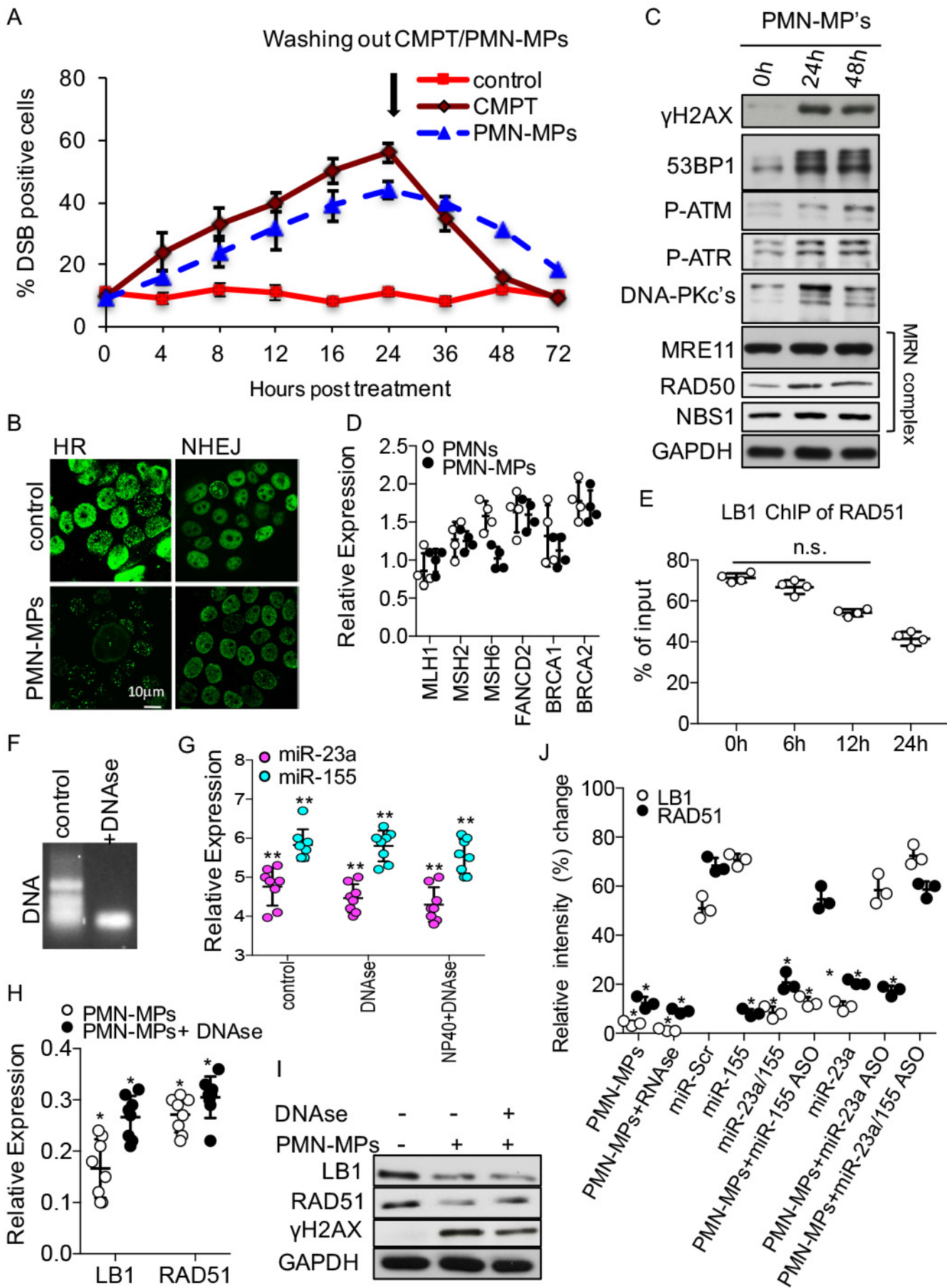
1. Butin-Israeli V, Houser MC, Feng M, Thorp EB, Nusrat A, Parkos CA, et al. Deposition of microparticles by neutrophils onto inflamed epithelium: a new mechanism to disrupt epithelial intercellular adhesions and promote transepithelial migration. *FASEB journal : official publication of the Federation of American Societies for Experimental Biology*. 2016;30(12):4007-20.
2. Adam SA, Butin-Israeli V, Cleland MM, Shimi T, and Goldman RD. Disruption of lamin B1 and lamin B2 processing and localization by farnesyltransferase inhibitors. *Nucleus*. 2013;4(2):142-50.
3. Moir RD, Montag-Lowy M, and Goldman RD. Dynamic properties of nuclear lamins: lamin B is associated with sites of DNA replication. *The Journal of cell biology*. 1994;125(6):1201-12.
4. Li J, Zhao Y, Lu Y, Ritchie W, Grau G, Vadas MA, et al. The Poly-cistronic miR-23-27-24 Complexes Target Endothelial Cell Junctions: Differential Functional and Molecular Effects of miR-23a and miR-23b. *Mol Ther Nucleic Acids*. 2016;5(8):e354.
5. Goldgraben MA, Russell R, Rueda OM, Caldas C, and Git A. Double-stranded microRNA mimics can induce length- and passenger strand-dependent effects in a cell type-specific manner. *RNA*. 2016;22(2):193-203.
6. Li X, Liu X, Xu W, Zhou P, Gao P, Jiang S, et al. c-MYC-regulated miR-23a/24-2/27a cluster promotes mammary carcinoma cell invasion and hepatic metastasis by targeting Sprouty2. *The Journal of biological chemistry*. 2013;288(25):18121-33.
7. Karkeni E, Astier J, Tourniaire F, El Abed M, Romier B, Gouranton E, et al. Obesity-associated Inflammation Induces microRNA-155 Expression in Adipocytes and Adipose Tissue: Outcome on Adipocyte Function. *J Clin Endocrinol Metab*. 2016;101(4):1615-26.
8. Chandran PA, Keller A, Weinmann L, Seida AA, Braun M, Andreev K, et al. The TGF-beta-inducible miR-23a cluster attenuates IFN-gamma levels and antigen-specific cytotoxicity in human CD8(+) T cells. *Journal of leukocyte biology*. 2014;96(4):633-45.
9. Caballero-Garrido E, Pena-Philippides JC, Lordkipanidze T, Bragin D, Yang Y, Erhardt EB, et al. In Vivo Inhibition of miR-155 Promotes Recovery after Experimental Mouse Stroke. *J Neurosci*. 2015;35(36):12446-64.
10. Pena-Philippides JC, Caballero-Garrido E, Lordkipanidze T, and Roitbak T. In vivo inhibition of miR-155 significantly alters post-stroke inflammatory response. *J Neuroinflammation*. 2016;13(1):287.
11. Zhou Q, Gallagher R, Ufret-Vincenty R, Li X, Olson EN, and Wang S. Regulation of angiogenesis and choroidal neovascularization by members of microRNA-23~27~24 clusters. *Proceedings of the National Academy of Sciences of the United States of America*. 2011;108(20):8287-92.
12. Jahid S, Sun J, Edwards RA, Dizon D, Panarelli NC, Milsom JW, et al. miR-23a promotes the transition from indolent to invasive colorectal cancer. *Cancer Discov*. 2012;2(6):540-53.

13. Shimi T, Butin-Israeli V, Adam SA, Hamanaka RB, Goldman AE, Lucas CA, et al. The role of nuclear lamin B1 in cell proliferation and senescence. *Genes & development*. 2011;25(24):2579-93.
14. Laemmli UK. Cleavage of structural proteins during the assembly of the head of bacteriophage T4. *Nature*. 1970;227(5259):680-5.
15. Shi SR, Shi Y, and Taylor CR. Antigen retrieval immunohistochemistry: review and future prospects in research and diagnosis over two decades. *The journal of histochemistry and cytochemistry : official journal of the Histochemistry Society*. 2011;59(1):13-32.
16. Olive PL, and Banath JP. The comet assay: a method to measure DNA damage in individual cells. *Nature protocols*. 2006;1(1):23-9.
17. Butin-Israeli V, Adam SA, Jain N, Otte GL, Neems D, Wiesmuller L, et al. Role of lamin b1 in chromatin instability. *Molecular and cellular biology*. 2015;35(5):884-98.
18. Furman JL, Mok PW, Badran AH, and Ghosh I. Turn-on DNA damage sensors for the direct detection of 8-oxoguanine and photoproducts in native DNA. *Journal of the American Chemical Society*. 2011;133(32):12518-27.
19. Butin-Israeli V, Adam SA, and Goldman RD. Regulation of nucleotide excision repair by nuclear lamin b1. *PloS one*. 2013;8(7):e69169.
20. Dutto I, Cazzalini O, Stivala LA, and Prosperi E. An improved method for the detection of nucleotide excision repair factors at local UV DNA damage sites. *DNA repair*. 2017;51:79-84.
21. Yokochi T, and Gilbert DM. Replication labeling with halogenated thymidine analogs. *Current protocols in cell biology / editorial board, Juan S Bonifacino [et al]*. 2007;Chapter 22:Unit 22 10.
22. Akyuz N, Boehden GS, Susse S, Rimek A, Preuss U, Scheidtmann KH, et al. DNA substrate dependence of p53-mediated regulation of double-strand break repair. *Molecular and cellular biology*. 2002;22(17):6306-17.
23. Keimling M, Volcic M, Csernok A, Wieland B, Dork T, and Wiesmuller L. Functional characterization connects individual patient mutations in ataxia telangiectasia mutated (ATM) with dysfunction of specific DNA double-strand break-repair signaling pathways. *FASEB journal : official publication of the Federation of American Societies for Experimental Biology*. 2011;25(11):3849-60.
24. Keimling M, Deniz M, Varga D, Stahl A, Schrezenmeier H, Kreienberg R, et al. The power of DNA double-strand break (DSB) repair testing to predict breast cancer susceptibility. *FASEB journal : official publication of the Federation of American Societies for Experimental Biology*. 2012;26(5):2094-104.

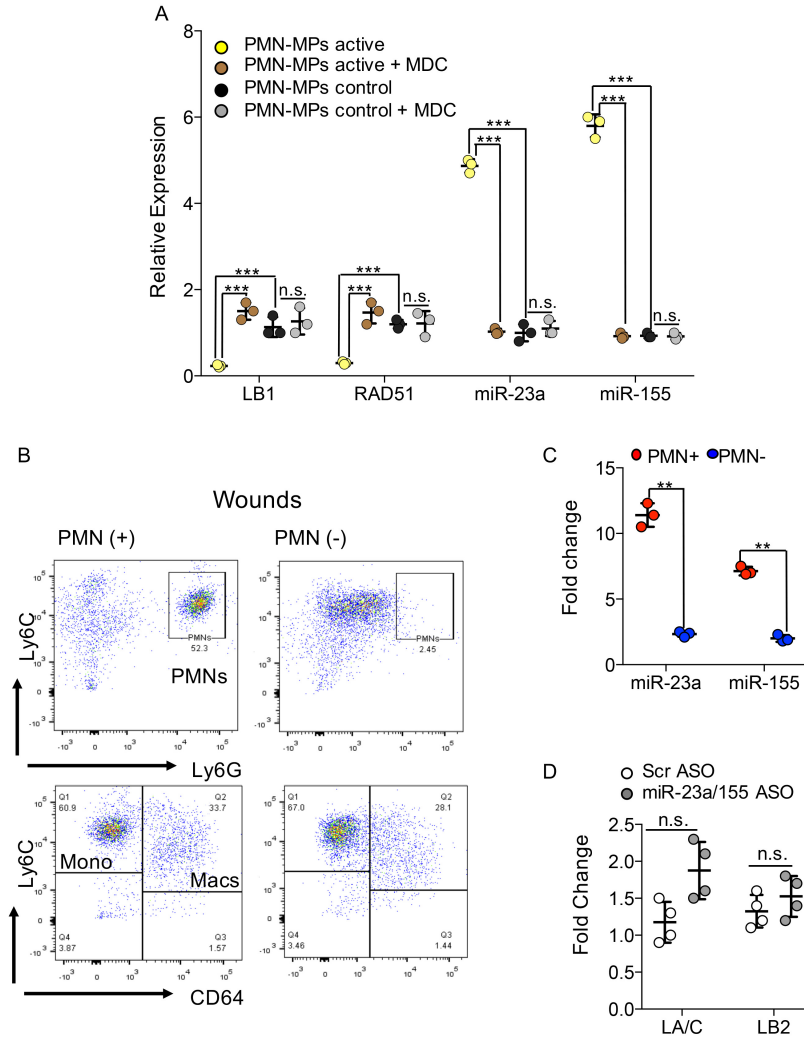
Sup Fig 1



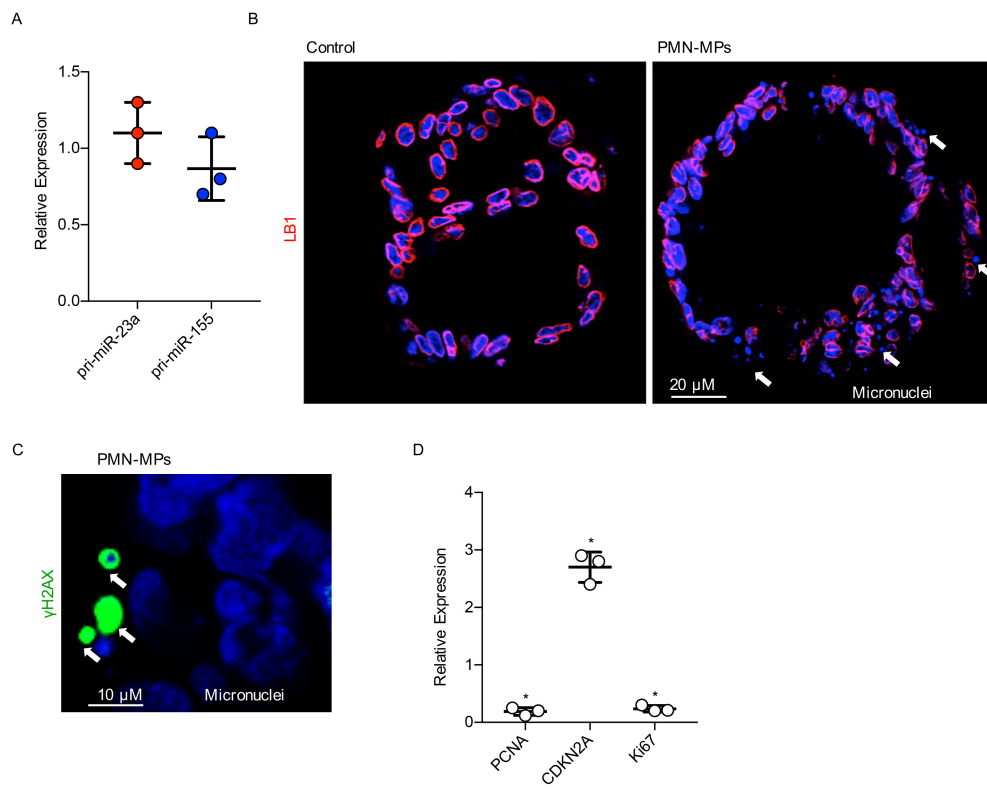
Sup Fig 2



Sup Fig 3



Sup Fig 4



Symbol	Pathway	DDR targets	Active PMNs	STDEV	PMN-MPs	STDEV	IBD A/NA	STDEV
miR-9	TNF α , cell migration, EMT	HR: BRCA1	6.2*	2.1	2.8*	0.3	8.2*	2.2
miR-21	IL-6; TNF α , cell migration	MMR: MSH2, MSH6	5.8*	2.2	2.5*	1.1	3.8*	1.4
miR-506	Carcinogenesis	HR: RAD51	4.1	2.8	2.2	1.8	2.3	0.5
miR-103	Oxidative stress, carcinogenesis	HR: RAD51	7.9*	2.2	0.6	0.1	3.2	2.1
miR-101	Wnt signaling, cell adhesion	DDR/HR: ATM NHEJ: DNA-PKcs	1.5	0.4	0.6	0.2	0.8	0.2
miR-34a	TP53 signaling, cell cycle, apoptosis, carcinogenesis	DDR signaling: 53BP1; TP53	1.5	0.2	0.7	0.2	2.9*	0.4
miR-24	Cell migration, invasion	DDR: H2AX, BRCA1	0.9	0.3	0.6	0.2	2.3	1.7
miR-146a	TLR/ NF κ B signaling	HR: BRCA1,	1.8	0.6	1.2	0.2	3.8	2.2
miR-124	Stem-cell renewal, differentiation	DDR: PARP-1; NHEJ: Ku70	2.4	0.7	1.2	0.4	1.9	0.9
Let-7	Stress response	HR: BRCA1/2	4.3	2.2	0.8	0.1	2.8	1.4
miR-23a	Carcinogenesis; CRC; EMT	HR: FANCG Nuclear stability: LBI	7.3*	1.1	4.7*	0.8	7.2*	2.1
miR-155	Pro-inflammatory; TNF α /TGFB/IFN γ	MMR: MSH1, MSH6, MLH2, RAD51	8.1*	2.7	5.2*	1.2	5.2*	2.5
pri-miR-23a			9*	0.5	0.7	0.2	5.3*	0.9
pri-miR-155			9.8*	0.6	0.9	0.1	6.7*	1.2

Sup Table 1. Expression of DNA damage repair regulating miRNA by PMN and PMN-MPs. Expression analyses of pro-inflammatory miRNAs associated with detection and repair of DNA damage were performed by qRT-PCR for the following conditions: 1. FMLF-stimulated PMNs (1 μ M, 20 min, 37 $^{\circ}$ C), 2. MPs isolated from FMLF-stimulated PMNs, 3. Fresh clinical biopsies of active IBD (A) and healthy (non-inflamed, NA) colonic tissue. U-6 was used as a reference gene. Significance was set if expression change was > 2.1 or < 0.5. All of the results presented are the mean \pm standard deviation from at least three separate experiments.